INTERNATIONAL JOURNAL OF CLIMATOLOGY
Int. J. Climatol. (2017)
Published online in Wiley Online Library
(wileyonlinelibrary.com) DOI: 10.1002/joc.5260

Royal Meteorological Society

Synoptic classification in 21st century CMIP5 predictions over the Eastern Mediterranean with focus on cyclones

Assaf Hochman,[a,b,c]* Tzvika Harpaz,[a,c] Hadas Saaroni[a,c] and Pinhas Alpert[a]
[a] *Department of Geophysics, School of Geosciences, Tel-Aviv University, Israel*
[b] *Department of Geography and the Human Environment, School of Geosciences, Tel-Aviv University, Israel*
[c] *Porter School of Environmental Studies, School of Geosciences, Tel-Aviv University, Israel*

ABSTRACT: The Mediterranean has been recognized as a 'hot spot', currently influenced by climate change, and predicted to be strongly affected in the future by significant warming and drying. This trend is expected to be expressed in changes in the occurrence and intensity of Mediterranean cyclones, in general, and of East Mediterranean (EM), i.e. Cyprus Lows (CL), in particular, as well as in the occurrence of all other synoptic systems dominating the region.

Here we have modified the semi-objective synoptic classification (Alpert *et al.*, 2004) to investigate future changes in the occurrence of EM synoptic types, with an emphasis on CLs. The modified classification was applied to eight CMIP5 models for the present (1986–2005), mid-21st century (2046–2065) and end of the century (2081–2100) periods, for both RCP4.5 and RCP8.5 scenarios.

The modified classification captured the synoptic-type frequencies for the present period well, and particularly excelled in capturing that of the CLs. For the future period, approximately a 35% reduction in CL occurrence is found towards the end of the 21st century (RCP8.5). Analysing this reduction for each of the seven specific types of CLs showed that lows located to the west of Cyprus are the main contributors to this decrease. The reductions in the frequencies of CLs are accompanied by an increase in the frequencies of Red Sea Troughs in winter. The predicted changes in the occurrence of various synoptic types in general and of CLs, in particular, will lead to a more accurate forecast of local potential climatic hazards.

KEY WORDS CMIP5; synoptic classification; Cyprus Lows; cyclones; Eastern Mediterranean

Received 4 April 2017; Revised 2 July 2017; Accepted 1 August 2017

1. Introduction

The Mediterranean has been recognized as one of the regions which is currently being significantly affected by climate change, defined as a 'hot spot', and is predicted to be influenced in the future by warming and drying (Giorgi, 2006; IPCC, 2013; Lelieveld *et al.*, 2016). Moreover, a tendency towards extremes was also observed, along with a seemingly contradicting change in the Mediterranean rainfall regime: an increase in extreme daily rainfalls and a decrease in the total amounts of rainfall (Alpert *et al.*, 2002; IPCC, 2013; Westra *et al.*, 2013).

Among the natural processes affecting this region are synoptic-scale phenomena such as Mediterranean cyclones (Lionello *et al.*, 2010, 2014). A unique characteristic of the Mediterranean region is the coexistence of different kinds of cyclones. Indeed, in spite of their generally limited size and duration, Mediterranean cyclones are known to have a prominent impact on the highly populated coastal areas surrounding the basin, due to the associated strong winds and heavy precipitation. The majority of intense Mediterranean storms show a baroclinic life cycle typical of mid-latitudes extra-tropical cyclones (Flaounas *et al.*, 2015). However, under specific conditions, a few storms evolve into tropical-like cyclones (Cavicchia *et al.*, 2014). The majority of extreme weather events in the Mediterranean are associated with intense cyclones (Nissen *et al.*, 2010, 2014).

Large-scale systems, such as the North Atlantic Oscillation, are suggested to contribute to Mediterranean cyclogenesis (Raible, 2007) along with other large-scale perturbations, e.g. the extension of the Asian monsoon and the Red Sea Trough (Fita *et al.*, 2006; Claud *et al.*, 2010; Flaounas *et al.*, 2015; Krichak *et al.*, 2016). The occurrence of cyclones in the Mediterranean exhibits a spatial pattern characterized by several maxima (Alpert *et al.*, 1990; Trigo *et al.*, 1999; Lionello *et al.*, 2016). The most intense cyclogenesis area is located in the Gulf of Genoa in the northwest. Another cyclogenetic area begins south of the Atlas mountain ridge and enters the central part of the basin from southwest. Other areas of increased cyclone activity are located in the North Aegean Sea and the Black Sea. The signature of the Cyprus Lows (CL) is found in the Levantine Basin.

CLs are mid-latitude disturbances that tend to develop in the Levantine Basin when upper troughs or cut-off lows penetrate the EM (Zangvil *et al.*, 2003). CLs transport cool air, originating from Eastern Europe, over the

* Correspondence to: A. Hochman, Department of Geophysics, School of Geosciences, Tel-Aviv University, Tel-Aviv 69978, Israel. E-mail: assafhochman@post.tau.ac.il

Table 1. List of synoptic types/groups and their abbreviations (Alpert *et al.*, 2004).

Synoptic group	Abbreviation	English name
Lows	Lw	cold Low to the West of Cyprus
	CL_N-D	Cyprus Low to the North (Deep)
	CL_N-S	Cyprus Low to the North (Shallow)
	CL_S-D	Cyprus Low to the South (Deep)
	CL_S-S	Cyprus Low to the South (Shallow)
	L_E-D	Low to the East (Deep)
	L_E-S	Low to the East (Shallow)
Red Sea Troughs	RST_E	Red Sea Trough with an Eastern axis
	RST_C	Red Sea Trough with a Central axis
	RST_W	Red Sea Trough with a Western axis
Persian Troughs	PT-W	Persian Trough (Weak)
	PT-M	Persian Trough (Medium)
	PT-D	Persian Trough (Deep)
Highs	H_W	High to the West
	H_E	High to the East
	H_N	High to the North
	H_C	High over Israel (Central)
Sharav Lows	SL_W	Sharav Low to the West of Israel
	SL_C	Sharav Low over Israel (Central)

warmer Mediterranean where it becomes moist and unstable (Alpert and Reisin, 1986; Shay-El and Alpert, 1991; Saaroni *et al.*, 2010a). These lows contribute 90% of the annual precipitation in Israel (Goldreich, 2003; Goldreich *et al.*, 2004). The rainfall yield and its spatial distribution over Israel are highly sensitive to the location of a CL (Zangvil *et al.*, 2003).

The synoptic patterns of the Levant region are described by the semi-objective synoptic classification (SC) of Alpert *et al.* (2004). This classification was found to well express the local weather conditions, especially for atmospheric disturbances as CLs (Saaroni *et al.*, 2010a, 2010b; Dayan *et al.*, 2012). Alpert *et al.* (2004) showed a decrease in the occurrences of CLs in the second part of the 20th century due to global warming. Saaroni *et al.* (2010a) used the products of the SC (Alpert *et al.*, 2004) to investigate the effect of the intensity (depth) and location of the seven types of CLs (hence forth, CL types) on daily precipitation distribution in Israel. Raible *et al.* (2010) using outputs of climate models showed that the frequency of cyclones in the western and middle parts of the Mediterranean basin is projected to decrease in the 21st century, while no significant change is predicted in the EM. There is a large spread among the models and tracking methods concerning variability and trends of cyclones (Raible *et al.*, 2010; Nissen *et al.*, 2014; Zappa *et al.*, 2015).

The purpose of this study is to investigate the changes in the frequencies of synoptic types over the EM (for list of synoptic types, see Table 1), with an emphasis on CL types, using a SC approach.

2. Data

Data were acquired from the National Center for Environmental Prediction/National Center for Atmospheric Research (NCEP/NCAR) reanalysis archive (Kalnay *et al.*, 1996; Kistler *et al.*, 2001). This database is available on daily and 6 h timescales from 1948 to the present on a $2.5° \times 2.5°$ spatial resolution. Modelled data were retrieved from the World Data Center for Climate (WDCC-DKRZ, http://cera-www.dkrz.de/WDCC/ui/Index.jsp) data portal for eight models participating in the fifth phase of the Coupled Model Inter-comparison Project (CMIP5, for list of models see Table 2). The main improvements in CMIP5 with respect to CMIP3 include the addition of interactive ocean and land carbon cycles, more comprehensive modelling of the indirect effect of aerosols and the use of volcanic and solar forcing in most models (Taylor *et al.*, 2012). Models data are available on daily and 6 h timescales for 1861–2100. Spatial resolutions vary in range from $0.94° \times 1.25°$ to $3.71° \times 3.75°$ (Table 2). CMIP5 models constitute closely related simulations distinguished by the triad of integers formatted as $r<N>i<M>p<L>$ (e.g. r1i1p1). In this study, all of the simulations come from the same initialization method ('i1') and same 'perturbed physics' parameterization ('p1'). The same realizations ('r') were generally used for historical and future scenarios (Tables S1 and S2, Supporting Information). This is recommended for drawing a fluent time line between historical and future simulations (Taylor *et al.*, 2012). However, for analysing decadal distributions for synoptic groups it is not as essential and the models spread is much larger than the individual members of each model (Appendix) (Taylor *et al.*, 2012; Sillman *et al.*, 2013).

Table 2. The eight CMIP5 models in the present study with the following listing columns: modelling centre (or group), institute ID, model name, and horizontal resolution (°) following Taylor *et al.* (2012).

Modelling centre (or group)	Institute ID	Model name (short name)	Resolution (°)
Canadian Centre for Climate Modelling and Analysis, Canada	CCCMA	CanESM2 (CANESM)	2.79×2.81
National Center for Atmospheric Research, USA	NCAR	CCSM4 (CCSM)	0.94×1.25
Met Office Hadley Centre, England	MOHC	HadGEM2-CC (HadGEM2CC)	1.25×1.88
		HadGEM2-ES (HadGEM2ES)	1.25×1.88
Institut Pierre-Simon Laplace, France	IPSL	IPSL-CM5A-LR (IPSL)	1.9×3.75
Max Planck Institute for Meteorology, Germany	MPI-M	MPI-ESM-LR (MPI)	1.87×1.88
Meteorological Research Institute, Japan	MRI	MRI-CGCM3 (MRI)	1.12×1.13
Norwegian Climate Center, Norway	NCC	NORESM1-M (NORESM)	1.9×2.5

The analysis is based on the historical (1986–2005) simulations of the CMIP5 models and NCEP/NCAR reanalysis. Future periods simulated are mid-21st century (2046–2065) and end century (2081–2100) for RCP4.5 and RCP8.5 scenarios, following the recommendation of the Fifth Assessment Report (AR5) of the Intergovernmental Panel on Climate Change (IPCC, 2013). The representative concentration pathways (RCP) adopted by the IPCC for its fifth assessment report (AR5) are RCP2.6, RCP4.5, RCP6 and RCP8.5. They are named after the possible radiative forcing (e.g. RCP2.6 refers to an increase of 2.6 W m^{-2}) expected in the year 2100 relative to pre-industrial values. RCP2.6 assumes that the global greenhouse gas (GHG) emissions will peak between 2010 and 2020 and then will decline, RCP4.5 assumes GHG will peak around 2040, RCP6 assumes GHG will peak around 2080 and RCP8.5 assumes that GHG will continue to rise throughout the 21st century.

3. Method

To predict the changes in synoptic-type distributions in the future, the SC algorithm used by Alpert *et al.* (2004) was applied to the above mentioned CMIP5 models, with the only difference being the input variables. While Alpert *et al.* (2004) used geopotential height, temperature and wind components at 1000 hPa (12Z), models data (except for SLP – sea level pressure) were used at 850 hPa instead due to lack of hourly data in 1000 hPa (12Z) outputs. The hourly data are a prerequisite for the SC algorithm of Alpert *et al.* (2004). Moreover, the purpose here was to minimize the difference between the original algorithm and the modified one. It should be noted that the models' data are available in a variety of spatial resolutions (Table 2), therefore were linearly interpolated to fit the required 25 grid points (27.5°–37.5°N; 30°–40°E) used by Alpert *et al.* (2004).

The change in input variables and its effect on the synoptic-type occurrences was verified for the historical period (1986–2005). This was done by a comparison between the original SC applied to NCEP/NCAR reanalysis and the modified one applied to the CMIP5 models, using Taylor diagrams (Taylor, 2001). A Taylor diagram can provide a concise statistical summary of how well patterns match each other in terms of their correlation, their root-mean-square difference and the ratio of their variances. This approach evaluates the ability of the models to capture the 19 weather patterns. Figure 1 shows the Taylor diagrams for annual [Figure 1(a), all types; Figure 1(b), CL types] and winter (DJF) [Figure 1(c), all types; Figure 1(d), CL types]. The distribution of CLs (Figures 1(b) and (d)) in CMIP5 was found to significantly resemble the distribution of CLs in NCEP/NCAR reanalysis, since these lows are well pronounced and can easily be detected by the algorithm, even at a different pressure level, i.e. 850 hPa instead of 1000 hPa. The comparison done for the distribution of all synoptic types during the winter (Figure 1(c)) remains significant because of the dominance of lows during these months. Figure 1(a) shows that the change between pressure levels, in the original *versus* the modified SC, influences mainly the annual distributions.

It should be expected that using inputs from 850 hPa pressure level instead of the original 1000 hPa pressure level would over/under estimate the cold/warm low-pressure systems, since cold/warm low-pressure systems tend to deepen/shallow with height, respectively (Holton, 2004). Therefore, this change does not influence the analysis for CLs, which is the focus of this study.

It was concluded that the modified SC determines synoptic-type occurrences well, especially for CL. Thus, the modified SC was applied to CMIP5 models for mid-century (2046–2065) and end of the century (2081–2100) periods.

4. Results

Figure 2 summarizes the CMIP5 projections (RCP4.5 and RCP8.5) of annual CL frequency for the 21st century. A significant (Table S1) CL decreasing trend is observed in all models, more pronounced in the harsh scenario (RCP8.5, on average −34.4%). All CL types contribute to this decrease (Table S1) except for the CLs to the south of Israel, which constitute less than 0.5% of all days. Figure 3 summarizes the CMIP5 average ensemble projections (RCP4.5 and RCP8.5) of annual synoptic group frequencies (in % of all days: Lows, CL; RST, Red Sea Troughs; PT, Persian Troughs; H, Highs) for the 21st century. As expected, over/underestimation of the cold/warm CL/PT, respectively, is shown for the CMIP5 models ensemble (850 hPa) with respect to the original NCEP classification (1000 hPa). The high-pressure synoptic group is replicated well by the ensemble of the models. It is shown that the decreasing trend in CLs is accompanied by significant increasing trends in PTs and some RST increases. The PTs (weak and medium) are the main contributors to these increases (~150% increase on average, Table S1). These types of PTs were associated with heat extremes during the summer in the EM (Ziv *et al.*, 2005; Lelieveld *et al.*, 2016). PTs increase may be associated with the enhancement of the warm season of the year because of global warming (to be shown in a following study).

Figure 4 summarizes the CMIP5 projections (RCP4.5 and RCP8.5) of winter (DJF) CL frequency for the 21st century. The significant decreasing (Table S2) trend in winter resembles the annual one (Table S1). However, the main contributor to this decreasing trend, during winter, is the cold low to the west of Cyprus (Lw). On average, the occurrence of this type of cyclone decreases by −33.6% (Table S2). Lw is formed when cold air from the north moves over the warmer Mediterranean Sea. These cyclones are considered as frontal cyclones, while the more eastern CL types are generated by the local synergistic effects of topography (Anatolian high) and sea heat fluxes (Alpert *et al.*, 1995). Mediterranean Sea surface temperatures are expected to increase in the future. Hence, the

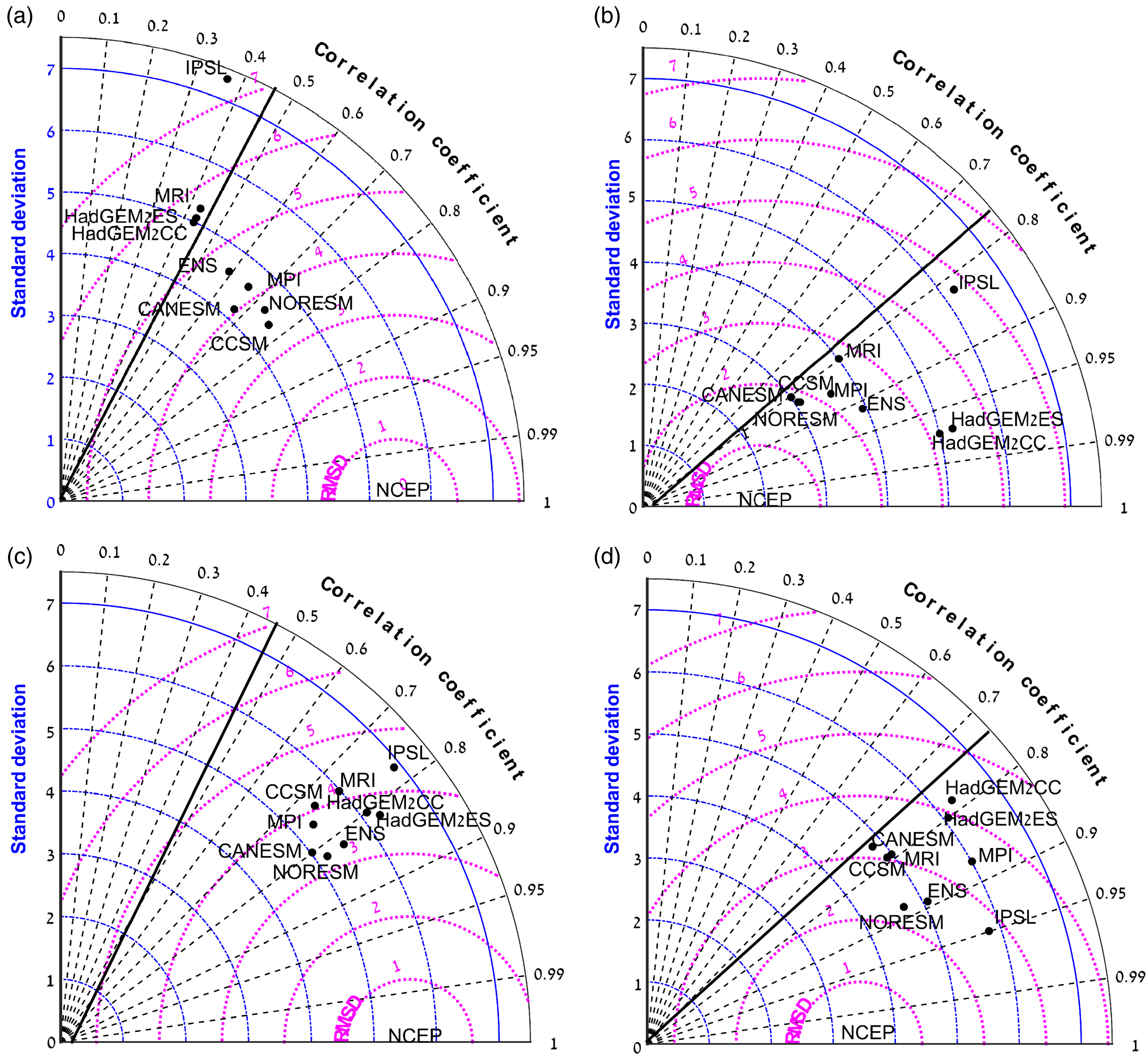

Figure 1. Taylor diagrams of CMIP5 (classified with 850hPa_uwind, 850 hPa _vwind, 850 hPa _T and SLP) compared with original (Alpert *et al.*, 2004) NCEP/NCAR (classified with 1000 hPa: uwind, vwind, T and GPH) synoptic types historic (1986–2005) occurrences. (a) Annual 19 synoptic types; (b) annual 7 Cyprus Low types; (c) winter (DJF) 19 synoptic types; (d) winter (DJF) 7 Cyprus Low types. The correlations are significant at the 95% level under a two tailed *t*-test, for correlations that are higher than the solid black line. [Colour figure can be viewed at wileyonlinelibrary .com].

predicted decrease in the occurrence of Lw might be due to a weakening of upper cold air intrusions from the north along with the expected expansion of the Hadley Cell towards the Poles in a warmer climate (Lu *et al.*, 2007).

Figure 5 summarizes the CMIP5 average ensemble projections (RCP4.5 and RCP8.5) of winter synoptic group frequencies. An expected over/under estimation of the cold/warm CL/RST, respectively, is shown for the CMIP5 models ensemble (850 hPa) with respect to the original NCEP classification (1000 hPa). The CMIP5 ensemble accurately replicates the high-pressure systems and the absence of PTs. The decreasing trend in CLs is accompanied by increases in both RSTs and Highs (Figure 5 and Table S2). The main contributor to the increase in RST occurrences is the RST with a central axis (RSTc), for which seven of the models show significant increases (73.3% on average) in its occurrence at the end of the century. Although the RST is a low-pressure system, it is usually not an active weather system in terms of precipitation, and was associated with intense air pollution days in the region (Saaroni *et al.*, 2009).

5. Summary and conclusions

The change in EM cyclones frequency and intensity is a central question in predicting of future hazardous weather phenomena in the region. A SC approach was applied to investigate the changes in the occurrence of synoptic types in the EM, with special emphasis on CL. The

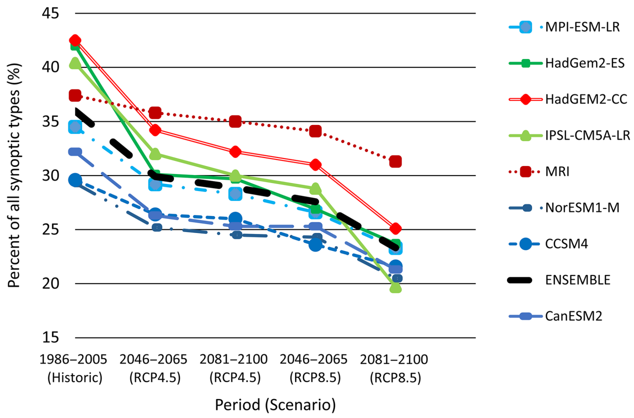

Figure 2. CMIP5 annual Cyprus Low frequencies for the historic (1986–2005), mid-century (2046–2065) and end of the century (2081–2100) periods for RCP4.5 and RCP8.5 scenarios. Significance levels are shown in Table S1. [Colour figure can be viewed at wileyonlinelibrary.com].

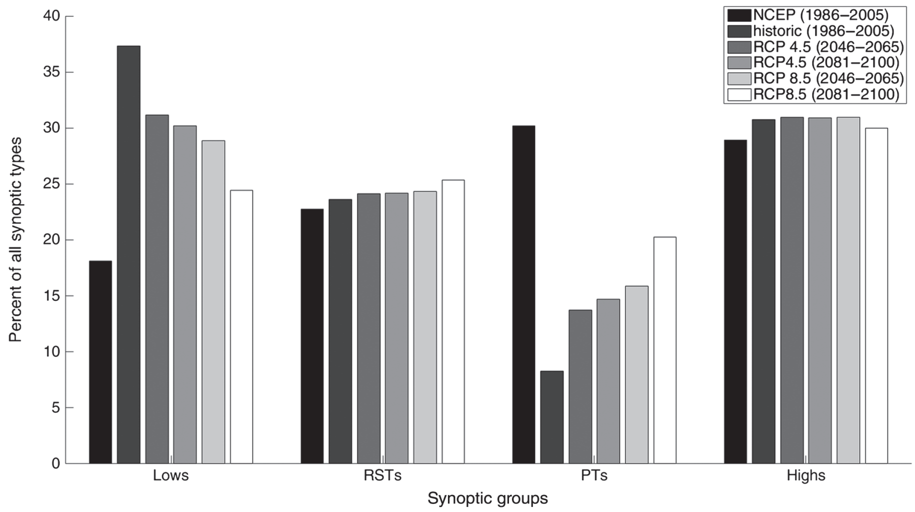

Figure 3. The eight CMIP5 models average ensemble of annual synoptic group frequencies (in %: Lows, Cyprus Lows; RST, Red Sea Troughs; PT, Persian Troughs; H, Highs) for the historic (1986–2005), mid-century (2046–2065) and end of the century (2081–2100) periods for RCP4.5 and RCP8.5 scenarios. The NCEP synoptic classification is shown for reference. Significance levels are shown in Table S1.

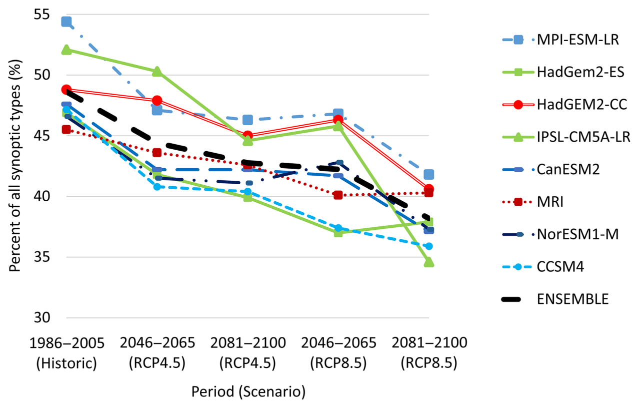

Figure 4. Same as Figure 2, but for the winter (DJF) season. Significance levels are shown in Table S2. [Colour figure can be viewed at wileyonlinelibrary.com].

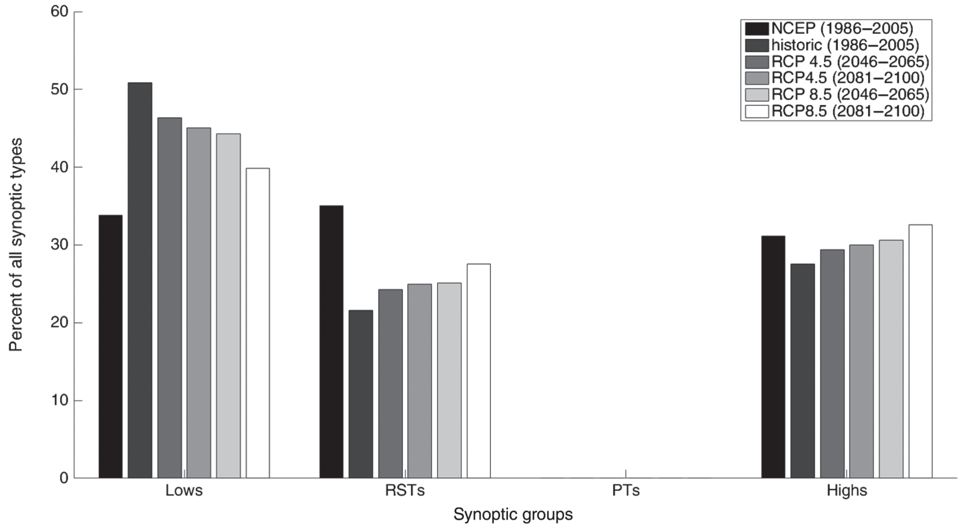

Figure 5. Same as Figure 3, but for the winter (DJF) season. Significance levels are shown in Table S2.

early semi-objective SC (Alpert *et al.*, 2004) was modified, applied to eight CMIP5 models, and the results were evaluated for the historical simulations (1986–2005). It was shown that the modified classification captured significantly well the occurrence of the different synoptic types and excelled in capturing CLs.

It is concluded that for the RCP8.5/RCP4.5 scenarios, a reduction in the frequency of CLs is expected, of ~35 and ~22%, from 37 to 24% of the days and from 37 to 29% of the days annually, by the end of the 21st century, respectively (Figure 3). These reductions are shown here to be compensated by increases in PTs and RSTs on an annual and winter season temporal resolution, respectively. Intriguing is the significant reduction in the cold low to the west of Cyprus (Lw), which may be explained by a reduction in the intrusions of cold air masses aloft and the predicted expansion of the Hadley Cell towards the poles. Although the intensity of CLs was not investigated here, it can be assumed that the expected reductions in total annual precipitation can be at least in part, the result of changing synoptic weather patterns in the EM. The projected intensity of CLs is a subject of further research.

Finally, the predicted changes in the occurrence of various synoptic types in general and of CLs, in particular, will lead to a more accurate forecast of local potential climatic hazards, associated with these weather patterns.

Acknowledgements

We would like to thank the editor and anonymous reviewers for their valuable time and useful contributions. The inputs suggested by the reviewers definitely helped improve our manuscript. We thank the Ministry of Science and Technology of Israel and Tel-Aviv University president and Mintz Foundation for their support. This study was also partially supported by cooperation in the international virtual institute DESERVE (Dead Sea Research Venue), funded by the German Helmholtz Association and by the Porter School of Environmental Studies at Tel-Aviv University.

Appendix

The triad of integers formatted as $r < N > i < M > p < L >$ (e.g. r1i1p1) distinguish between closely related simulations by a single CMIP5 model. CMIP5 historical runs initialized from different times of a control run would be identified by the ‘realization’ number ‘r1’, ‘r2’, ‘r3’, and so on. While future model outputs are named after the historical run that created their initial state, e.g. a future model with ‘r1’ was initialized by an ‘r1’ historical run. It is recommended to use products of similar historical and future runs, but for the purposes of synoptic group frequencies it has a small effect, as shown below. To evaluate the effect of different ‘realizations’ ‘r’ on the synoptic group frequencies in CMIP5 models, we evaluated the differences between r5i1p1 and r1i1p1 simulations of the CanESM2 model with respect to the synoptic classification algorithm of Alpert *et al.* (2004) for 1986–2005. This was done for: (1) the difference in Taylor diagram verification measures (correlation, standard deviation and root mean square difference; Table S3); and (2) the difference in synoptic group frequencies for the annual and winter (DJF) season temporal resolutions in models with the same ‘realizations’ (Figures S1(a) and (c)) and with different ‘realizations’ (Figures S1(b) and (d)). It was found that the difference between the two simulations is statistically insignificant (Table S3). Furthermore, the difference between the projections of synoptic group occurrences in the future was also found to be insignificant when using different ‘realizations’ simulations for the historical runs (Figure S1). It can be concluded that the effect of different ‘realizations’ (r) in the historical simulations as compared with the future RCP scenario simulations has a very small effect (if any) on the distribution of synoptic group occurrences for the CanESM2 model. The other two models which had different ‘realizations’ (Tables S1 and

S2) are assumed to follow similar results. Furthermore, the differences between the models are much larger than the differences between the specific models simulations (Sillman *et al.*, 2013).

Supporting information

The following supporting information is available as part of the online article:

Table S1. CMIP5 models (RCP4.5 and RCP8.5) synoptic type annual frequency projections (in % of all types) for the historical (1986–2005), mid-century (2046–2065) and end of the century (2081–2100) periods. Significance tested at 95% confidence and power levels under a two tailed binomial distribution. *Compared to 1986–2005; **compared to 2046–2065.

Table S2. Same as Table S1 but for the winter (DJF) season.

Table S3. Verification measures for CanESM2 historical r1i1p1 and r5i1p1 for winter (DJF) and annual temporal resolutions.

Figure S1. A comparison between synoptic group occurrences of the five models (MPI-ESM-LR, HadGEM2-ES, HadGEM2-CC, NorESM1-M and CCSM4) that had the same 'realizations' ('r') for historical and future simulations (a, b: annual; c, d: winter) and the same models with additional three models (IPSL_CM5A_LR, CanESM2 and MRI_CGCM3) without the same 'realizations' ('r').

References

Alpert P, Reisin T. 1986. An early winter polar air mass penetration to the eastern Mediterranean. *Mon. Weather Rev.* **114**: 1411–1418.

Alpert P, Neeman BU, Shay-El Y. 1990. Climatological analysis of Mediterranean cyclones using ECMWF data. *Tellus* **42A**: 65–77.

Alpert P, Stein U, Tsidulko M. 1995. Role of sea fluxes and topography in eastern Mediterranean cyclogenesis. *Glob. Atmos. Ocean Syst.* **3**: 55–79.

Alpert P, Ben-Gai T, Baharad A, Benjamini Y, Yekutieli D, Colacino M, Diodato L, Ramis C, Homar V, Romero R, Michaelides S, Manes A. 2002. The paradoxical increase of Mediterranean extreme daily rainfall in spite of decrease in total values. *Geophys. Res. Lett.* **29**(11): 31-1–31-4. https://doi.org/10.1029/2001GL013554.

Alpert P, Osetinsky I, Ziv B, Shafir H. 2004. Semi-objective classification for daily synoptic systems: application to the Eastern Mediterranean climate change. *Int. J. Climatol.* **24**: 1001–1011.

Cavicchia L, von Storch H, Gualdi S. 2014. Mediterranean tropical-like cyclones in present and future climate. *J. Clim.* **27**: 7493–7501.

Claud C, Alhammoud B, Funatsu BM, Chaboureau JP. 2010. Mediterranean hurricanes: large-scale environment and convective and precipitating areas from satellite microwave observations. *Nat. Hazards Earth Syst. Sci.* **10**: 2199–2213.

Dayan U, Tubi A, Levy I. 2012. On the importance of synoptic classification methods with respect to environmental phenomena. *Int. J. Climatol.* **32**: 681–694.

Fita L, Romero R, Ramis C. 2006. Intercomparison of intense cyclogenesis events over the Mediterranean basin based on baroclinic and diabatic influences. *Adv. Geosci.* **7**: 333–342.

Flaounas E, Raveh-Rubin S, Wernli H, Drobinski P, Bastin S. 2015. The dynamical structure of intense Mediterranean cyclones. *Clim. Dyn.* **44**: 2411–2427.

Giorgi F. 2006. Climate change hot spots. *Geophys. Res. Lett.* **33**: L08.

Goldreich Y. 2003. *The Climate of Israel: Observation, Research and Application*. Springer: New York, 298 pp.

Goldreich Y, Moses H, Rosenfeld D. 2004. Radar analysis of cloud systems and their rainfall yield in Israel. *Isr. J. Earth Sci.* **53**: 63–76.

Holton J. 2004. *Introduction to Dynamic Meteorology*. Elsevier Academic Press: New York, 531 pp.

IPCC. 2013. *Climate Change 2013: The Physical Science Basis. Contribution of Working Group I to the Fifth Assessment Report of the Intergovernmental Panel on Climate Change*, Stocker TF, Qin D, Plattner GK, Tignor M, Allen SK, Boschung J, Nauels A, Xia Y, Bex V, Midgley PM (eds). Cambridge University Press: Cambridge, UK and New York, NY, 1535 pp. https://doi.org/10.1017/CBO9781107415324.

Kalnay E, Kanamitsu M, Kistler R, Collins W, Deaven D, Gandin L, Iredell M, Saha S, White G, Woollen J, Zhu Y, Chelliah M, Ebisuzaki W, Higgins W, Janowiak J, Mo KC, Ropelewski C, Wang J, Leetmaa A, Reynolds R, Jenne R, Joseph D. 1996. The NCEP/NCAR 40-year reanalysis project. *Bull. Am. Meteorol. Soc.* **77**: 437–471.

Kistler R, Kalnay E, Collins W, Saha S, White G, Woollen J, Chelliah M, Ebisuzaki W, Kanamitsu M, Kousky V, Van Den Dool H, Jenne R, Fiorino M. 2001. The NCEP-NCAR 50-year reanalysis: monthly means CD-ROM and documentation. *Bull. Am. Meteorol. Soc.* **82**: 247–267.

Krichak SO, Feldstein SB, Alpert P, Gualdi S, Scoccimaro E, Yano JI. 2016. Discussing the role of tropical and subtropical moisture sources in extreme precipitation events in the Mediterranean region from a climate change perspective. *Nat. Hazards Earth Syst. Sci.* **16**: 269–285.

Lelieveld J, Proestos Y, Hadjinicolaou P, Tanarhte M, Tyrlis E, Zittis G. 2016. Strongly increasing heat extremes in the Middle East and North Africa (MENA) in the 21st century. *Clim. Change* **137**: 245–260. https://doi.org/10.1007/s10584-016-1665-6.

Lionello P, Cavaleri L, Nissen KM, Pinto C, Raicich F, Ulbrich U. 2010. Severe marine storms in the Northern Adriatic: characteristics and trends. *Phys. Chem. Earth* **40**: 93–105.

Lionello P, Abrantes F, Gacic M, Planton S, Trigo R, Ulbrich U. 2014. The climate of the Mediterranean region: research progress and climate change impacts. *Reg. Environ. Change* **14**: 1679–1684.

Lionello P, Trigo IF, Gil V, Liberato ML, Nissen KM, Pinto JG, Raible CC, Reale M, Tanzarella A, Trigo RM, Ulbrich S. 2016. Objective climatology of cyclones in the Mediterranean region: a consensus view among methods with different system identification and tracking criteria. *Tellus A* **68**: 29391. https://doi.org/10.3402/tellusa.v68.29391.

Lu J, Vecchi GA, Reichler T. 2007. Expansion of the Hadley cell under global warming. *Geophys. Res. Lett.* **34**: L06805. https://doi.org/10.1029/2006GL028443.

Nissen KM, Leckebusch GC, Pinto JG, Renggli D, Ulbrich S, Ulbrich U. 2010. Cyclones causing wind storms in the Mediterranean: characteristics, trends and links to large-scale patterns. *Nat. Hazards Earth Syst. Sci.* **10**: 1379–1391.

Nissen KM, Leckebusch GC, Pinto JG, Ulbrich U. 2014. Mediterranean cyclones and windstorms in a changing climate. *Reg. Environ. Change* **14**: 1873–1890.

Raible CC. 2007. On the relation between extremes of mid-latitude cyclones and the atmospheric circulation using ERA40. *Geophys. Res. Lett.* **34**: L07703. https://doi.org/10.1029/2006GL029084.

Raible CC, Ziv B, Saaroni H, Wild M. 2010. Winter synoptic-scale variability over the Mediterranean Basin under future climate conditions as simulated by the ECHAM5. *Clim. Dyn.* **35**: 473–488.

Saaroni H, Ziv B, Uman T. 2009. Does a synoptic classification indicate the NO_x pollution potential? The case of the metropolitan area of Tel-Aviv, Israel. *Water Air Soil Pollut.* **207**: 139–155.

Saaroni H, Halfon N, Ziv B, Alpert P, Kutiel H. 2010a. Links between the rainfall regime in Israel and location and intensity of Cyprus Lows. *Int. J. Climatol.* **30**: 1014–1025.

Saaroni H, Ziv B, Osetinsky I, Alpert P. 2010b. Factors governing the inter-annual variation and the long-term trend of the 850-hPa temperature over Israel. *Q. J. R. Meteorol. Soc.* **136**: 305–318.

Shay-El Y, Alpert P. 1991. A diagnostic study of winter diabatic heating in the Mediterranean in relation to cyclones. *Q. J. R. Meteorol. Soc.* **117**: 715–747.

Sillman J, Kharin VV, Zhang X, Zwiers FW, Bronaugh D. 2013. Climate extreme indices in the CMIP5 multi-model ensemble. Part 1: model evaluation in the present climate. *J. Geophys. Res.* **118**: 1716–1733.

Taylor KER. 2001. Summarizing multiple aspects of model performance in a single diagram. *J. Geophys. Res.* **106**(D7): 7183–7192.

Taylor KER, Stouffer J, Meehl GA. 2012. An overview of CMIP5 and the experiment design. *Bull. Am. Meteorol. Soc.* **93**: 485–498.

Trigo IF, Davies TD, Bigg GR. 1999. Objective climatology of cyclones in the Mediterranean region. *J. Clim.* **12**: 1685–1696.

Westra S, Alexander L, Zwiers F. 2013. Global increasing trends in annual maximum daily precipitation. *J. Clim.* **26**: 3904–3918.

Zangvil A, Karas S, Sasson A. 2003. Connection between Eastern Mediterranean seasonal mean 500 hPa height and sea-level pressure patterns and the spatial rainfall distribution over Israel. *Int. J. Climatol.* **23**: 1567–1576.

Zappa G, Hawcroft MK, Shaffrey L, Back E, Brayshaw D. 2015. Extratropical cyclones and the projected decline of winter Mediterranean precipitation in the CMIP5 models. *Clim. Dyn.* **45**: 1727–1738. https://doi.org/10.1007/s00382-014-2426-8.

Ziv B, Saaroni H, Baharad A, Yekutieli D, Alpert P. 2005. Indications of aggravation of summer heat conditions over the Mediterranean basin. *Geophys. Res. Lett.* **32**: L12706. https://doi.org/10.1029/2005GL022796.

